The anharmonic phonon decay rate in group-III nitrides

2009 J. Phys.: Condens. Matter 21 174205

(http://iopscience.iop.org/0953-8984/21/17/174205)

IOP PUBLISHING JOURNAL OF PHYSICS: CONDENSED MATTER

J. Phys.: Condens. Matter **21** (2009) 174205 (8pp) doi:10.1088/0953-8984/21/17/174205

The anharmonic phonon decay rate in group-III nitrides

G P Srivastava

School of Physics, University of Exeter, Stocker Road, Exeter EX4 4QL, UK

Received 8 September 2008, in final form 10 November 2008
Published 1 April 2009
Online at stacks.iop.org/JPhysCM/21/174205

Abstract

Measured lifetimes of hot phonons in group-III nitrides have been explained theoretically by considering three-phonon anharmonic interaction processes. The basic ingredients of the theory include full phonon dispersion relations obtained from the application of an adiabatic bond charge model and crystal anharmonic potential within the isotropic elastic continuum model. The role of various decay routes, such as Klemens, Ridley, Vallée–Bogani and Barman–Srivastava channels, in determining the lifetimes of the Raman active zone-centre longitudinal optical (LO) modes in BN (zincblende structure) and A_1(LO) modes in AlN, GaN and InN (wurtzite structure) has been quantified.

(Some figures in this article are in colour only in the electronic version)

1. Introduction

It is widely known that crystal anharmonicity plays an important role in determining thermal properties of solids, such as thermal expansion and thermal conductivity. Crystal anharmonicity also plays an important role in controlling the lifetime of hot phonons which are generated during energy relaxation of carriers in semiconductors. In semiconductor devices electrons are highly excited into conduction band either optically or by applying electric field. These high energy carriers decay towards their ground state, largely by emission of (near) zone-centre optical phonons [1]. When the excited carrier density is large, the optical phonon emission can be very fast with an eventual non-equilibrium population. The hot phonon effect, caused by slow dissipation (i.e. long lifetime) of optical phonons, causes degradation of device performance. The reduction factor in carrier energy relaxation mechanism has been estimated [2] to be up to 40 in GaAs, 20 in GaN and 24 in InN. For an efficient carrier relaxation in technologically important semiconductors, such as group-III nitrides, it is important that the generated optical phonons are rapidly mutated or dissipated.

Damping of longitudinal optical (LO) modes in polar cubic semiconductors has been studied experimentally both in frequency domain using spontaneous Raman spectroscopy [3–7], and in time domain using incoherent anti-Stokes Raman scattering [8, 9] and time-resolved coherent anti-Stokes Raman scattering (CARS) [10–12]. The hot phonon effect starts to take place when the phonon lifetime exceeds carrier lifetime (in the low sub-picosecond range). From Raman spectroscopic measurements [13–15] it has been revealed that the hot phonon effect is present for zone-centre LO modes in the wurtzite phase of GaN and InN.

From theoretical view point, the lifetime of the phonons generated during carrier relaxation in semiconductors can be controlled by various sources such as impurity scattering, carrier scattering, and anharmonic scattering from other phonons. For high quality single crystals phonon–impurity scattering can be neglected. Also, observed phonon lifetimes (in the ps range) are usually much larger than that predicted from carrier–phonon interaction (in the fs range) [16]. Thus it is assumed that lifetime of such phonons is almost exclusively contributed by anharmonic interactions in the form of decay into phonons of lower energies. For grown samples, however, the low temperature phonon lifetimes may also be influenced by roughness scattering.

In order to calculate phonon lifetimes governed by anharmonic interactions we require three main ingredients: (i) Fourier transform of crystal anharmonic potential, (ii) phonon dispersion relation and (iii) a full-scale numerical scheme for Brillouin zone integration. Earlier theoretical attempts relied on making huge simplifications for each of these points. Such simplifications include: a simple expression for crystal anharmonic term based on an ad hoc treatment, linear dispersion relations for acoustic phonon branches and Debye's isotropic continuum model for Brillouin zone integration. The second and third of these simplifications can to some extent be expected to work for semiconductors

in the cubic phase (diamond and zincblende structures with two atoms per unit cell) but not in non-cubic phases (such as the wurtzite structure with four atoms per unit cell). In addition to the consideration of acoustic branches, a proper account must be made of phonon dispersion relations for low-lying optical branches in the wurtzite structure of group-III nitrides. First detailed calculations of anharmonic phonon decay in cubic semiconductors with a clear understanding of different decay mechanisms were made by Debernardi and co-workers [17, 18]. However, their approach, based on a first-principles treatment of all the three ingredients mentioned above, is very demanding both from the theoretical and computational view points. Their method will become even more demanding for group-III nitrides in the wurtzite structure. In addition to being computationally very intensive, their method is not yet fully tested for determining the ingredient (i), namely the Fourier transform of anharmonic crystal potential.

Over the past few years we have made a systematic study of phonon lifetimes in cubic and hexagonal semiconductors by employing the Debye model, with crystal anharmonicity incorporated in the spirit of an isotropic elastic continuum scheme [19, 20]. Although some useful insight was gained, that theory cannot be expected to present accurate and unbiased predictive results. More recently, we have adopted a middle of the road approach in determining the lifetime of LO modes in hexagonal group-III nitrides [21]. This approach considers the ingredients (ii) and (iii) fully and accurately, and treats the ingredient (i) in a physically appealing and consistent manner. In this work we explain our approach fully and present results for the lifetime of the LO mode in zincblende BN and for the A_1 (LO) mode in wurtzite AlN, GaN and InN. We attempt to explain both the magnitude and temperature variation of experimentally observed results by using three-phonon processes. We also point out the most influential decay channels for each of these nitride materials.

2. Theory

2.1. Anharmonicity and phonon decay rate

Let us represent a phonon mode as $\mathbf{q}s$, where $\mathbf{q}$ is the wavevector and s is the polarization index. Treating a crystal as an isotropic anharmonic elastic continuum, the cubic part of crystal anharmonicity can be expressed as [22]

$$V_3 = \frac{1}{3!}\sqrt{\frac{\hbar^3}{2\rho N_0 \Omega}} \sum_{\mathbf{q}s\mathbf{q}'s'\mathbf{q}''s''} F_3(\mathbf{q}s)\sqrt{\omega(\mathbf{q}s)\,\omega(\mathbf{q}'s')\,\omega(\mathbf{q}''s'')} \times (a^\dagger_{\mathbf{q}s} - a_{-\mathbf{q}s})(a^\dagger_{\mathbf{q}'s'} - a_{-\mathbf{q}'s'})(a^\dagger_{\mathbf{q}''s''} - a_{-\mathbf{q}''s''})\,\delta_{\mathbf{q}+\mathbf{q}'+\mathbf{q}'',\mathbf{G}}, \quad (1)$$

where ρ is the material density, N_0 is the number of unit cells, Ω is the volume per unit cell, $\omega(\mathbf{q}s)$, $\omega(\mathbf{q}'s')$ and $\omega(\mathbf{q}''s'')$ are frequencies of phonons modes $\mathbf{q}s$, $\mathbf{q}'s'$, $\mathbf{q}''s''$, $\mathbf{G}$ is a reciprocal lattice vector, and $a^\dagger_{\mathbf{q}s}$, $a_{\mathbf{q}s}$ etc are the phonon creation and annihilation operators, respectively. The coefficient $F_3(\mathbf{q}s)$ can be expressed in terms of second- and third-order elastic constants, and is mode and temperature dependent. In addition, this coefficient is expected to take a specific value for each three-phonon interaction process the mode $\omega(\mathbf{q}s)$ undergoes [22, 23]. Instead of using a complicated and unreliable expression for $F_3(\mathbf{q}s)$ we will treat it in the form of a mode-average and temperature dependent adjustable parameter $\mathcal{F}$. Within the elastic continuum model this parameter can be expressed as $\mathcal{F} = \gamma/\bar{c}$, where γ is mode-averaged but temperature dependent Grüneisen's constant and $\bar{c}$ is average acoustic speed for phonons. While it is tempting to use this relationship and consider γ and $\bar{c}$ as two adjustable parameters, we feel that it is more convenient to treat the cubic anharmonic potential energy V_3 in terms of the single adjustable parameter $\mathcal{F}$.

Considering anharmonicity as perturbation to the harmonic part of crystal potential, we can apply Fermi's golden rule formula to derive expressions for three-phonon scattering events. We will consider a zone-centre phonon $(\mathbf{q} = \mathbf{0})s$ to decay most dominantly via the normal ($\mathbf{G} = \mathbf{0}$) three-phonon anharmonic interaction mechanism into two daughter modes $\mathbf{q}'s'$ and $\mathbf{q}''s''$: i.e. $(\mathbf{q} = \mathbf{0})s \rightarrow \mathbf{q}'s' + \mathbf{q}''s''$. Following [22], the decay rate can be expressed as

$$\tau^{-1}_{\mathbf{0}s} = \frac{\pi\hbar\mathcal{F}^2}{2\rho N_0 \Omega} \sum_{\mathbf{q}'s'\mathbf{q}''s''} \omega(0s)\,\omega(\mathbf{q}'s')\,\omega(\mathbf{q}''s'') \times \frac{\bar{n}(\omega(\mathbf{q}'s'))\,\bar{n}(\omega(\mathbf{q}''s''))}{\bar{n}(\omega(\mathbf{0}s))} \times \delta_{\mathbf{0},\mathbf{q}'+\mathbf{q}''}\,\delta(\omega(0s) - \omega(\mathbf{q}'s') - \omega(\mathbf{q}''s'')), \quad (2)$$

where $\bar{n}(\omega(\mathbf{0}s))$ etc represent the Bose–Einstein distribution function for the phonon modes $\mathbf{q}s$, etc.

2.2. Lattice dynamics

Realistic phonon dispersion relations in tetrahedrally semiconductors have been obtained from the application of both phenomenological and *ab initio* theories of lattice dynamics. Phenomenological approaches include the rigid ion model, shell models and adiabatic bond charge model. The adiabatic bond charge model, developed originally for zincblende semiconductors by Rustagi and Weber [24] and extended for wurtzite semiconductors by Tütüncü and Srivastava [25, 26], is among the most physically appealing and successful approaches for calculating the phonon dispersion relations for tetrahedrally bonded semiconductors, including group-III nitrides. The main idea in this model is that the valence electron charge density distribution is represented by massless bond charges, endowed with translational degrees of freedom. In III–V semiconductors the bond charges are positioned along atomic bonds, displayed towards anions with the ratio 3:5. Interatomic forces are derived from long-ranged Coulomb, short-ranged central and short-ranged non-central (i.e. bond-bending) Keating potentials.

The quality of the results for phonon eigensolutions obtained from the adiabatic bond charge model calculations matches that of *ab initio* calculations [27]. For zincblende BN there are three acoustic phonon branches and three optical phonon branches. For wurtzite AlN, GaN and InN, there are three acoustic branches, three low-lying optical branches, and six upper-lying optical branches. In this work we are interested in examining the anharmonic decay rate of the zone-centre LO

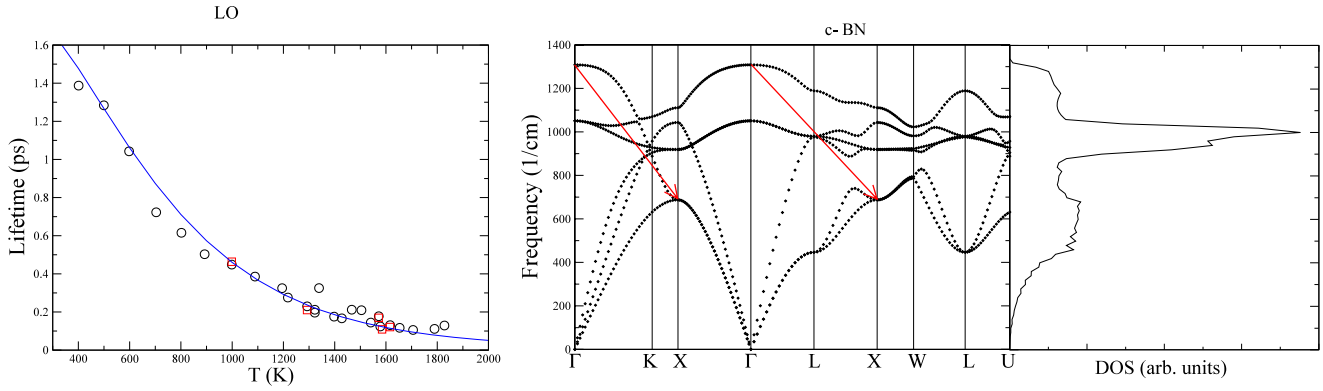

Figure 1. Phonon dispersion relations, density of states, and temperature variation of the anharmonic lifetime of the LO mode in zincblende BN. The dominant decay routes (via the Klemens channel) are indicated by arrows. The experimental lifetime results (shown by symbols) are taken from [37].

mode (the mode with the highest frequency) in zincblende BN and the A_1(LO) mode (the 11th zone-centre mode) for wurtzite AlN, GaN and InN.

2.3. Brillouin zone summation

Having discussed ingredients (i) and (ii) we now will describe our scheme to deal with ingredient (iii), namely the Brillouin zone summation necessary for evaluating the phonon decay rate using equation (2). Dealing with Brillouin zone summation is an essential requirement for realistic computation of any property of a crystalline solid. Over the past few decades many different schemes have been developed and applied with reasonable success. Some of the available schemes are inherently more computationally demanding than others. One of the newer schemes, which is now routinely applied in electronic band structure calculations, is based on the concept of 'special points' within an irreducible part of the central Brillouin zone of the lattice under consideration. According to this scheme, the zone average of a function $f(\mathbf{k})$ is obtained as

$$f(\mathbf{k}) = \sum_{i=1}^{M} w_i f(\mathbf{k}_i), \tag{3}$$

where $\{\mathbf{k}_i\}$ represents a set of M 'special points' and w_i is the weight factor associated with the point $\mathbf{k}_i$ subject to the normalization condition $\sum_i w_i = 1$. Several schemes exist for generating $\{\mathbf{k}_i\}$ and $\{w_i\}$.

For evaluating the expression in equation (2) we first choose to carry out the summation over $\mathbf{q}''$ by using the momentum conserving condition expressed by the Kronecker delta symbol. This fixes the condition $\mathbf{q}'' = -\mathbf{q}'$. The summation over $\mathbf{q}'$ is carried out by using the Monkhorst–Pack special points [28] obtained from the $10 \times 10 \times 10$ division of the FCC Brillouin zone and the $10 \times 10 \times 8$ division of the hexagonal Brillouin zone. The energy conservation condition in equation (2) was dealt with by converting the Dirac delta function to the Gaussian form with a small broadening factor. With the above considerations, and invoking the time reversal symmetry, equation (2) reduces to

$$\tau_{\mathbf{0}s}^{-1} = \frac{\pi\hbar\mathcal{F}^2}{2\rho\Omega}\frac{1}{\sigma\sqrt{\pi}}\sum_{s',s''}\sum_{j=1}^{M} w_j\, \omega(\mathbf{q}'_j s')\, \omega(\mathbf{q}'_j s'') \times \frac{\bar{n}(\omega(\mathbf{q}'_j s'))\, \bar{n}(\omega(\mathbf{q}'_j s''))}{\bar{n}(\omega(\mathbf{0}s))} \times \exp\left[-\left(\frac{\omega(0s) - \omega(\mathbf{q}'_j s') - \omega(\mathbf{q}'_j s'')}{\sigma\ \omega(0s)}\right)^2\right], \tag{4}$$

where σ represents the Gaussian broadening factor.

3. Results and discussion

3.1. Phonon dispersion relations

We will first note some important features of the phonon dispersion relations (namely ω versus $\mathbf{q}$ curves) and the resulting vibrational density of states $g(\omega)$ for zincblende BN and wurtzite AlN, GaN and InN.

Figure 1 shows the calculated phonon dispersion curves and the vibrational density of states for zincblende BN along several symmetry directions in the FCC Brillouin zone. Due to similar masses of the B and N atoms, there is no clear separation between the acoustic and optical branches. It is clear that the consideration made in the Debye model of linear dispersion relation for the acoustic branches is valid only in the long wavelength regime. Also, the density of states in the acoustic range is significantly different from the quadratic variation with frequency, i.e. it does not show the behaviour $g(\omega) \propto \omega^2$ for the entire part of the acoustic range, a feature commonly employed in the Debye model. Actually, the density of states is constant in the upper acoustic frequency range 425–675 cm^{-1}. The dispersion relation and the corresponding density of states in the optical range show non-simple features. There is a sharp and reasonably narrow peak in the density of states at around the frequency 950 cm^{-1}, namely in the transverse optical range.

The phonon dispersion curves and vibrational density of states for wurtzite structure AlN, GaN and InN are shown in figures 2–4 along various symmetry directions in the hexagonal Brillouin zone. As discussed in our

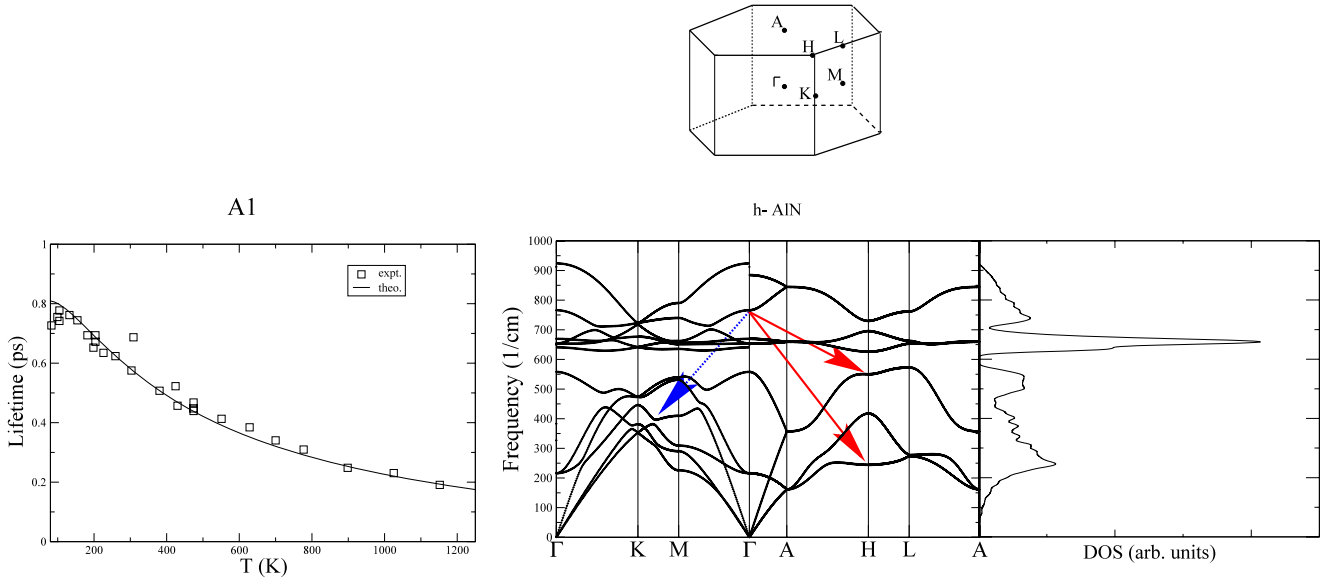

Figure 2. Phonon dispersion relations, density of states, and temperature variation of the anharmonic lifetime of the A_1(LO) mode in wurtzite AlN. The dominant decay routes (via the Ridley and Barman–Srivastava channels) are indicated by arrows. The experimental lifetime results (shown by symbols) are taken from [14].

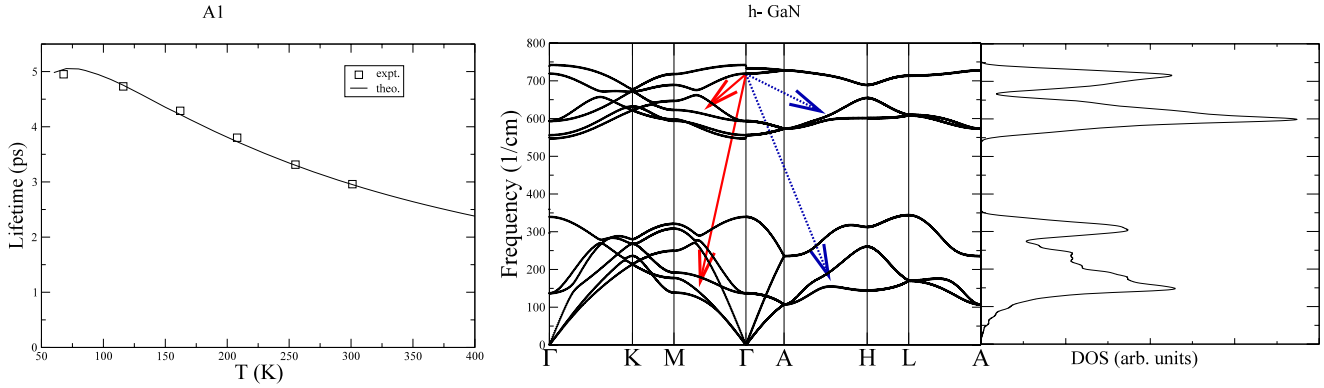

Figure 3. Phonon dispersion relations, density of states, and temperature variation of the anharmonic lifetime of the A_1(LO) mode in wurtzite GaN. The dominant decay routes (via the Ridley channel) are indicated by arrows. The experimental lifetime results (shown by symbols) are taken from [13].

previous publications [25, 26], these results agree very well with experimental measurements [29] and first-principles theoretical calculations [27, 30]. Group theoretical analysis of phonon modes [29] suggests that at the centre of the hexagonal Brillouin zone the highest Raman active mode is of symmetry A_1(LO). This mode is indicated as the tip of the arrows drawn in figures 2–4.

Due to the difference in the masses of Al and N atoms, the higher-lying optical branches in AlN are separated from the continuum of other branches with a small gap of approximately 50 cm^{-1}. Below the gap there are two broad peaks in the density of states curve, centred 250 and 525 cm^{-1}. Above the gap there is a sharp peak at 650 cm^{-1} and a small peak at 750 cm^{-1}. The density of states shows the Debye-like quadratic behaviour only up to about 250 cm^{-1}. For GaN, due to a larger mass difference between Ga and N, there is a larger gap of approximately 200 cm^{-1} between the upper-lying optical branches and the remaining branches. Below the gap, there are two main peaks at 150 and 300 cm^{-1}. Above the gap there are two sharp peaks at 600 and 700 cm^{-1}. The Debye-like variation of the density of states is only valid up to 100 cm^{-1}. The main features in the dispersion curves and density of states for InN are similar to those for GaN, except for some changes that occur due to the larger mass difference between In and N. The gap between the upper-lying and lower-lying optical branches has increased to approximately 225 cm^{-1}. Peaks in the density of states curve occur at 100 and 200 cm^{-1} below the gap and at 500 and 570 cm^{-1} above the gap. The Debye-like variation of the density of states is only valid up to 100 cm^{-1}.

3.2. General considerations for calculations of phonon decay rates

The frequency and temperature dependence of $\tau_{\mathbf{0}s}^{-1}$ due to cubic anharmonicity can be established analytically by performing

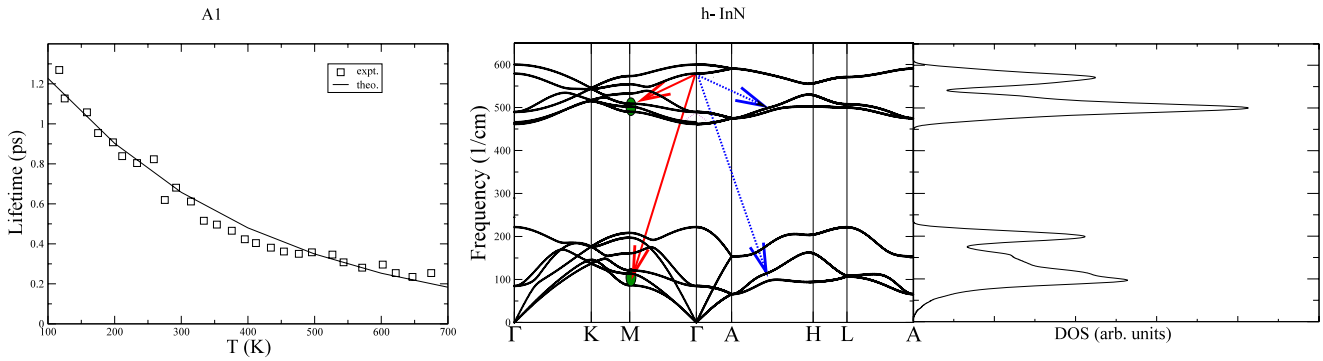

Figure 4. Phonon dispersion relations, density of states, and temperature variation of the anharmonic lifetime of the A_1(LO) mode in wurtzite InN. The dominant decay routes (via the Ridley and Barman–Srivastava channels) are indicated by arrows. The experimental lifetime results (shown by symbols) are taken from [15].

the sums in equation (2) within the isotropic continuum approximation. This was done in [20]. From the analytic expressions obtained in [20], and assuming γ to be temperature independent, it can be easily deduced that the anharmonic decay of a zone-centre phonon mode (of frequency ω) shows the following frequency and temperature dependences

$$\tau^{-1}(\omega, T) \propto \omega^5 \exp(-\alpha\omega/T) \qquad \text{at low temperatures}$$
$$\propto \omega^4 T \qquad \text{at high temperatures,} \tag{5}$$

where α is a constant. At very low temperatures the term $\exp(-\alpha\omega/T)$ can be approximated as a constant of temperature (close to unity), and the cubic anharmonic decay becomes 'spontaneous'. At high temperatures the decay rate increases linearly with temperature.

In our previous theoretical investigations [20], using the isotropic continuum approach and ignoring impurity/defect scattering, we concluded that the use of a single Grüneisen constant γ was insufficient to explain the temperature dependence of phonon lifetime over the temperature range for which the Raman data is available. Further effort (unpublished) has revealed that unacceptable temperature variation of γ would need to be considered in order to reproduce experimental data. Motivated by this, one of the objectives of this work is to investigate if a realistic temperature dependence of the coefficient $\mathcal{F}$, within the present theoretical approach based on a realistic phonon dispersion relations, can help explain the Raman results over the available temperature range. The need for including defect scattering to explain experimental results has already been recognized in previous works (such as in [15]). To achieve our overall aim, we note that three general considerations are required before attempting to apply the theory presented in this work to interpret and explain Raman measurement, and make further predictions regarding the magnitude and temperature variation of the lifetime of long wavelength non-equilibrium phonons in group-III nitrides. These are: (i) type and quality of sample, (ii) magnitude and temperature dependence of the cubic anharmonic coefficient $\mathcal{F}$, and (iii) possible role of higher-order anharmonicity (such as the contribution from four-phonon processes). If the sample contains impurities or defects, or is characterized by surface roughness, additional phonon scattering rate τ^{-1}(defect) must be included in the theory. Such scattering is temperature independent but can produce a dominant contribution to the total phonon scattering rate at low temperatures. In group-III nitrides, the role of such scattering can be important up to 400–500 K. The anharmonic phonon scattering coefficient $\mathcal{F}$ is expected to depend on temperature. This can be appreciated by relating $\mathcal{F}$ to the Grüneisen constant γ. Several works have verified that γ depends of temperature. In particular, the work by Bruls *et al* [31] has suggested that for AlN the value of γ between 300 and 1600 K lies in the range 0.70 and 0.96. However, the low temperature dominance of τ^{-1}(defect) means that there is no real need for modelling the temperature dependence of $\mathcal{F}$ up to 300 K when seeking a theoretical fit to Raman data for group-III nitrides. The role of four-phonon processes can only be expected to be appreciable at very high temperatures. Up to moderately high temperatures the phonon relaxation rate due to four-phonon processes is expected to be at least two orders of magnitude smaller than the rate due to three-phonon processes [32]. In the context of present investigations for group-III nitrides, we do not expect the relaxation rate of the LO mode in c-BN and the A_1(LO) mode in wurtzite AlN, GaN or InN to be contributed appreciably by four-phonon processes. With these considerations, we will attempt to explain the Raman measurements on the group-III nitride samples by including the effects (i) and (ii) described above.

The scattering rate of a phonon of frequency ω from impurities/defects/roughness can be calculated by using the Rayleigh formula $\tau^{-1}(\text{defect}) = A\omega^4$. The coefficient A will assume different form and values for different situations [33], and as the exact nature of defects, impurities, roughness of the samples studied here is not fully established, we will treat A as an adjustable parameter. As we have mentioned earlier, the cubic anharmonic parameter $\mathcal{F}$ can be considered to be related to the mode-average Grüneisen constant γ. Temperature variation of γ is rather difficult to establish, but it is expected to follow the following behaviour [34]

$$\gamma(T) = \gamma_0(1 + b\,T^2), \tag{6}$$

where γ_0 is a limiting low temperature value and b is an appropriate constant factor. Following this, we attempted the temperature variation of $\mathcal{F}$ in the form

$$\mathcal{F}(T) = \mathcal{F}(T_0)(1 + b\,(T - T_0)^2), \tag{7}$$

with $\mathcal{F}(T_0)$ fitted at a low temperature T_0. For group-III nitrides studied in this work, room temperature is a reasonably low temperature below which the effect of phonon scattering from impurities/defects can be expected to over-shadow any effect on the temperature variation of $\mathcal{F}$. Thus we have considered $T_0 = 300$ K as an appropriate choice.

3.3. Decay routes

As discussed in previous works in the literature, three decay routes are possible for the thermalization of the LO mode in cubic semiconductors with the diamond and zincblende structures. These are: (i) *Klemens channel* (decay into two acoustic modes) [35], (ii) *Vallée–Bogani channel* (decay into a lower mode of the same optical branch and an acoustic mode) [10, 11] and (iii) *Ridley channel* (decay into an optical mode of a lower branch and an acoustic mode) [36]. From the application of the diatomic linear chain model, it can be shown that the condition for the Klemens channel to be allowed on energy grounds is that the mass ratio of the constituent basis atoms does not exceed 3. In addition to these routes, there is an additional but very important channel for the decay of the A_1(LO) mode (and other modes) in hexagonal semiconductors, such as the wurtzite group-III nitrides. This is (iv) *Barman–Srivastava channel* (decay into two modes of lower optical branches) [20].

3.4. Decay rate of the LO mode in zincblende BN

Herchen and Cappelli [37] have presented the Raman data for the decay of the zone-centre LO mode in zincblende BN (i.e. c-BN). Their sample is single crystal with low impurity levels. In order to match our theoretical results with the experimental data there was no need to include any impurity/defect scattering of the phonon mode. However, following the discussion presented earlier, we attempted the temperature variation of $\mathcal{F}$ in the form given in equation (7). For zincblende BN we were able to fit the experimental Raman data between 300 and 1800 K by choosing $\mathcal{F}(T_0 = 300\ \text{K}) = 0.22 \times 10^{-4}$ m s^{-1} and $b = 0.65 \times 10^{-6}$ K^{-2}. Our calculated results for the decay rate between 300 and 2000 K are shown in the left panel of figure 1. Also shown are the experimental results of first-order Raman line widths, both Stokes and anti-Stokes, measured by Herchen and Cappelli [37]. The overall agreement between the theoretical and experimental results can be considered to be good.

An analysis of the computed results for the decay of the LO mode into TA, LA and TO branches suggests that 80% of the total contribution comes from the Klemens channel and the rest from the Ridley channel. The Vallée–Bogani channel is totally ineffective. The Klemens channel involves the possibility of the LO mode to decay into a combination of TA and LA modes. From our numerical results we find that the decays LO $\rightarrow$ TA + TA, LO $\rightarrow$ TA + LA and LO $\rightarrow$ TA + LA make the partial contributions of 80%, 10% and 10%, respectively, towards the Klemens channel. The most dominant of these, namely the decay of the LO mode into two TA modes, takes place at the X point within the Brillouin zone. This is indicated in figure 1.

In their work, Herchen *et al* [37] noted that the agreement between their theoretical results using a simple expression for three-phonon (or four-phonon) decay rate and the experimental results progressively worsened with the increase in temperature. To obtain good agreement between theory and experiment they had to include a combination of three-phonon and four-phonon decay rates. However, compared to three-phonon decay rate they had to use a much stronger decay rate contribution from four-phonon processes. This is in contrast to the generally accepted view that four-phonon processes are at least two orders of magnitude weaker than three-phonon processes. As we have shown from the application of the full theory, coupled with a reasonable temperature variation of the cubic anharmonic term $\mathcal{F}$, the decay of the LO mode can be explained entirely satisfactorily by only considering three-phonon processes.

3.5. Decay rate of the A_1LO mode in wurtzite AlN, GaN and InN

AlN. The results for the temperature variation, between 100 and 1200 K, of the A_1(LO) mode in wurtzite AlN are are shown in figure 2. At higher temperatures, consideration of only three-phonon processes was required to obtain good agreement between our numerical results and the time-resolved Raman measurements for bulk wurtzite AlN obtained by Kuball *et al* [14]. In doing so, we used equation (7) with the parameters $\mathcal{F}(T_0 = 100\ \text{K}) = 0.428 \times 10^{-4}$ s m^{-1} and $b = 0.2 \times 10^{-7}$ K^{-2}. In order to match our numerical results with the experimental results at low temperatures, we had to include an extra contribution from impurity/defect scattering of the A_1(LO) mode in the form $\tau^{-1}(\text{defect}) = A\omega^4 = 0.476 \times 10^{12}$ s^{-1}. Such a consideration is justified, as AlN is known to contain large amounts of unintentional oxygen-related impurities and defects [38]. In fact, due to the large affinity of AlN for oxygen, it is rather impossible to eliminate oxygen contamination.

The decay process is almost equally contributed by the Ridley channel and the Barman–Srivastava channel. In order to understand this we note that except for a small peak at around 225 cm^{-1}, the phonon density of states shows a broad structure up to around 550 cm^{-1}. The Ridley channel involves daughter phonons at and near the Brillouin zone point H (shown by the solid arrows in the middle panel of figure 2). The Barman–Srivastava channel involves daughter phonons along the K–M symmetry direction (shown by the dashed arrow in the figure). The Klemens and Vallée–Bogani channels are total ineffective.

GaN. Raman measurements of the decay rate of the A_1(LO) mode in wurtzite GaN have been made on samples prepared by MBE and CVD deposition techniques. Tsen *et al* [13] used an undoped MBE grown sample in the form of a 2 μm thick film with residual electron density approximately 10^{16} cm^{-3}, and density of photoexcited electron–hole pair about 5×10^{16} cm^{-3}. For this sample the room temperature decay rate of the A_1(LO) mode was observed to be 3.0 ps. In a later study Tsen *et al* [39] used an undoped CVD grown sample as a 6 μm thick film with plasma density 1×10^{16} cm^{-3}. For this sample the

measured room temperature decay rate of the A_1(LO) mode is 2.5 ps. The smaller decay rate in the more recent study can be expected to result from a slightly inferior quality of the CVD grown sample.

The results shown in the left panel of figure 3 are for the wurtzite GaN sample grown by Tsen *et al* [13] using molecular beam epitaxy (MBE). In order to match our theoretical results with available experimental data in the temperature range 50–300 K a temperature independent value of $\mathcal{F}(=0.208 \times 10^{-4}$ s m$^{-1})$ was found to be sufficient. However, in order to match low temperature experimental results for the MBE grown sample it was necessary to use phonon-defect scattering parameter in the form $\tau^{-1}(\text{defect}) = 0.0147 \times 10^{12}$ s^{-1}.

The dominant decay rate of the mode is governed by the Ridley channel involving daughter modes (particularly from the TA and higher-lying optical branches) along the Γ–M and A–H directions in the hexagonal Brillouin zone, as indicated in the middle panel of figure 3. Along both two directions there are flat phonon dispersion curves, leading to sharp peaks in the density of states at 150 cm^{-1} in the acoustic range and at 600 cm^{-1} in the upper optical range, as described earlier. The other decay channels are ineffective.

InN. Pomeroy *et al* [15] made Raman measurements on high quality MBE grown thin InN films. They reported the low temperature (100 K) lifetime of the A_1(LO) mode to increase from 0.75 to 1.3 ps with the film thickness increase from 0.25 to 7 μm. This clearly indicates the role of surface roughness on the lifetime. In addition, some contribution from phonon–impurity/defect can also be expected. With this in mind we have reproduced their experimental lifetime results for the InN film of thickness 7 μm in the temperature range 100–700 K by using $\tau^{-1}(\text{defect}) = 0.218 \times 10^{12}$ s^{-1} and three-phonon processes with the anharmonicity factor considered with the parameters $\mathcal{F}(T_0 = 100\ \text{K}) = 0.10 \times 10^{-4}$ s m^{-1} and $b = 0.12 \times 10^{-5}$ K^{-2}.

The A_1(LO) mode decays via both the Ridley and Barman–Srivastava channels, with the former making a dominant contribution. The Ridley channel takes place at two locations within the hexagonal Brillouin zone. One of the routes involves two daughter phonons of TA branches at/near the M point with energies around 80 cm^{-1} and of two of the higher-lying optical branches at around 500 cm^{-1}. Another route involves two daughter modes along the A-H symmetry direction, with frequencies approximately 100 cm^{-1} (transverse branches) and 480 cm^{-1} (up to four of the optical branches lying below the A_1 mode). The contribution from the Barman–Srivastava channel involves the two daughter phonons modes at/near the M point with frequencies at around 110 cm^{-1} (lowest-lying optical branch) and at around 489 cm^{-1} (lowest of the higher group of optical branches).

4. Summary and discussion

In this work we have presented a detailed account of the theory of anharmonic decay of a zone-centre phonon into two daughter phonons, with particular reference to group-III nitrides. It has been pointed out that consideration of realistic phonon dispersion relations, which in turn are governed by cation–anion mass ratio and interatomic force constants, plays an important role in determining effective decay routes. In order to present numerically accurate results we have used realistic phonon dispersion relations, an elastic continuum model for cubic anharmonicity, and an accurate scheme for Brillouin zone integration. The cubic anharmonic coupling constant is assumed to obey a temperature variation similar to that of the Grüneisen's constant.

We have successfully explained the available Raman measurements of the temperature variation of the lifetime of the LO mode in cubic BN and the A_1(LO) mode in hexagonal AlN, GaN and InN. The results have been explained in terms of contributions from various decay channels. In zincblende BN, for which the cation/anion mass ratio is $m_B/m_N = 0.77$, the Klemens channel (decay into two acoustic modes) and the Ridley channel (decay into an optical and an acoustic modes) contribute 80% and 20%, respectively. In wurtzite AlN, with $m_{Al}/m_N = 1.93$, there are almost equal contributions from the Ridley channel and the Barman–Srivastava channel (decay into two optical modes). In GaN, with $m_{Ga}/m_N = 4.98$, the entire contribution comes from the Ridley channel. In InN, with $m_{In}/m_N = 8.20$, the Ridley channel contributes a little more than the Barman–Srivastava channel.

At room temperature the lifetime results for the group-III nitrides are: 1.67 ps in BN, 0.58 ps in AlN, 2.96 ps in GaN and 0.66 ps in InN. We also note that experimentally measured low temperature results are approximately 0.8 ps, 5.0 ps and 1.2 ps for AlN, GaN and InN, respectively. The significantly low lifetime (i.e. fast decay rate) in AlN and InN results from the onset of the Barman–Srivastava channel. From our work we suggest that alloying GaN and/or InN with AlN would result in significant reduction in the 'hot phonon effect' observed in GaN and InN.

References

[1] Kash J, Hvam J, Tsang J C and Kuech T 1988 *Phys. Rev.* B **38** 5776
[2] Chen F, Cartwright A N, Lu H and Schaff W J 2003 *Appl. Phys. Lett.* **83** 4964 and references therein
[3] Chang R K, Ralston J M and Keating D E 1969 *Light Scattering Spectra of Solids* ed G B Wright (Berlin: Springer) p 369
[4] Kash J A, Jha S S and Tsang J C 1987 *Phys. Rev. Lett.* **58** 1869
[5] Bairamov B H, Ipatova I P, Milorava V A, Toporov V V, Naukkarinen K, Tuomi T, Irmer G and Monecke J 1988 *Phys. Rev.* B **38** 5722
[6] Bairamov B H, Voitenko V A, Ipatova I P, Negoduyko V K and Toporov V V 1994 *Phys. Rev.* B **50** 14 923
[7] Kernohan E T M, Philips R T, Bairamov B H, Ritchie D A and Simmons M Y 1996 *Solid State Commun.* **100** 263
[8] von der Linde D, Kuhl J and Klingenberg H 1980 *Phys. Rev. Lett.* **44** 1505
[9] Kash J A and Tsang J C 1992 *Spectroscopy of Nonequilibrium Electrons and Phonons* ed C V Shank and B P Zakharchenya (New York: Elsevier) p 113
[10] Vallée F and Bogani F 1991 *Phys. Rev.* B **43** 12049
[11] Vallée F 1994 *Phys. Rev.* B **49** 2460
[12] Bron W E, Kuhl J and Rhee B K 1986 *Phys. Rev.* B **34** 6961
[13] Tsen K T, Ferry D K, Botchkarev A, Sverdlov B, Salvador A and Morkoc H 1998 *Appl. Phys. Lett.* **72** 2132
[14] Kuball M, Hayes J M, Shi Y and Edgar J H 2000 *Appl. Phys. Lett.* **77** 1958

[15] Pomeroy J W, Kuball M, Lu H, Schaff W J, Wang X and Yoshikawa A 2005 *Appl. Phys. Lett.* **86** 223501
[16] Kash J A, Tsang J C and Hvam J M 1985 *Phys. Rev. Lett.* **54** 2151
[17] Debernardi A, Baroni S and Molinari E 1995 *Phys. Rev. Lett.* **75** 1819
[18] Debernardi A 1998 *Phys. Rev.* B **57** 12847
[19] Usher S and Srivastava G P 1994 *Phys. Rev.* B **50** 14179
[20] Barman S and Srivastava G P 2004 *Phys. Rev.* B **69** 235208
[21] Srivastava G P 2008 *Phys. Rev.* B **77** 155205
[22] Srivastava G P 1990 *The Physics of Phonons* (Bristol: Hilger)
[23] Ziman J M 1960 *Electrons and Phonons* (Oxford: Clarendon)
[24] Rustagi K C and Weber W 1976 *Solid State Commun.* **18** 673
[25] Tütüncü H M and Srivastava G P 2000 *Phys. Rev.* B **62** 5028
[26] Tütüncü H M, Srivastava G P and Duman S 2002 *Physica* B **316/317** 190
[27] Tütüncü H M, Bağcı S, Srivastava G P, Albudak A T and Ugur G 2005 *Phys. Rev.* B **71** 195309
[28] Monkhorst H J and Pack J D 1976 *Phys. Rev.* B **13** 5189
[29] Davydov V Yu, Kitaev Yu E, Goncharuk I N, Smirnov A N, Graul J, Semchinova O, Uffmann D, Smirnov M B, Mirgorodsky A P and Evarestov R A 1998 *Phys. Rev.* B **58** 12899
[30] Bungaro C, Rapcewicz K and Berholc J 2000 *Phys. Rev.* B **61** 6720
[31] Bruls R J, Hintzen H T, de With G, Metselaar R and van Miltenburg J C 2001 *J. Phys. Chem. Solids* **62** 783
[32] Ecsedy D J and Klemens P G 1977 *Phys. Rev.* B **15** 5957
[33] Klemens P G 1955 *Proc. Phys. Soc.* A **68** 1113
[34] Yates B 1972 *Thermal Expansion* (New York: Plenum)
[35] Klemens P G 1966 *Phys. Rev.* **148** 845
[36] Ridley B K 1996 *J. Phys.: Condens. Matter* **8** L511
[37] Herchen H and Cappelli M A 1993 *Phys. Rev.* B **47** 14193
[38] Slack G A 1973 *J. Phys. Chem. Solids* **34** 321
[39] Tsen K T, Kiang J G, Ferry D K and Morkoç H 2006 *Appl. Phys. Lett.* **89** 112111